Biomaterials Science

ROYAL SOCIETY OF CHEMISTRY

PAPER

View Article Online
View Journal

Cite this: DOI: 10.1039/d4bm01368a

Dimethysiloxane polymer for the effective transdermal delivery of donepezil in Alzheimer's disease treatment†

Jihyun Lee, ‡[a] In Gyoung Ju,‡[b] Yeon-Jin Lim,[c] Jin Hee Kim,[b] Seungmin Lee,[b] Yujin Choi,[b] Myung Sook Oh, *[b] Jaehoon Kim*[d] and Dokyoung Kim *[a,c,d,e,f,g]

Received 15th October 2024,
Accepted 19th November 2024

DOI: 10.1039/d4bm01368a

rsc.li/biomaterials-science

Donepezil (DNZ) has been used to treat dementia associated with mild, moderate, or severe Alzheimer's disease (AD). DNZ uptake can alleviate cognitive symptoms in AD patients *via* acetylcholinesterase (AChE) inhibition. However, oral administration of DNZ has limitations, including first-pass metabolism, difficulties with swallowing, and low patient compliance. In this work, we disclose a novel transdermal DNZ delivery system utilizing T2 polymer, synthesized *via* the ring-opening polymerization of 2,2,5,5-tetramethyl-2,5-disila-1-oxacyclopentane with trifluoroacetic acid (TFA). In the *in vivo* studies in an AD animal model, the DNZ-loaded T2 polymer (DNZ@T2) facilitated efficient transdermal DNZ delivery to the bloodstream and improved spatial working memory and long-term memory of the AD mouse model. Both the T2 polymer and DNZ@T2 exhibited low cytotoxicity and non-significant *in vivo* toxicity. This research highlights a promising transdermal delivery strategy for AD treatment, potentially enhancing therapeutic efficacy and patient compliance.

1. Introduction

The elderly population is on the rise globally, leading to an increase in patients suffering from neurodegenerative diseases such as Alzheimer's disease (AD).[1–4] To overcome AD, various treatment strategies are being introduced, including medications, lifestyle changes, cognitive therapy, supportive care, and advanced therapies such as gene therapy, stem cell therapy, and novel drug development.[5–10]

AD is characterized by progressive cognitive decline, beginning with symptoms such as short-term memory loss and disorientation.[11,12] These symptoms are closely related to decreased levels of acetylcholine (ACh) in the brain's neural circuit.[13,14] A certain level of ACh is crucial for memory formation and information processing.[15,16] However, in AD patients, acetylcholinesterase (AChE) leads to a reduction of ACh levels and subsequent cognitive decline.[17,18] Accordingly, AChE inhibitors, such as donepezil (DNZ), are used clinically to suppress AD symptoms.[17,19,20] DNZ can inhibit AChE activity, helping to maintain certain levels of ACh in the brain.[21–23] However, the oral administration of DNZ has several limitations: (1) it undergoes extensive first-pass metabolism in the liver, significantly diminishing its efficacy; (2) many AD patients have difficulty swallowing, which results in low medication adherence; (3) cognitive decline often leads to non-compliance with medication regimens, and (4) oral administration can become challenging due to increased behavioral issues in some patients.[24–27] In this context, developing new administration methods, such as transdermal delivery for AD patients has gained significant attention.[28,29] Transdermal administration offers several advantages, including bypassing the gastrointestinal tract and liver, thereby minimizing first-pass metabolism, enabling higher dosages, and maintaining more consistent plasma concentrations compared to traditional oral methods.[30–32] Furthermore, this method can reduce gastrointestinal disorders and side effects associated

[a]KHU-KIST Department of Converging Science and Technology, Kyung Hee University, Seoul 02447, Republic of Korea. E-mail: dkim@khu.ac.kr
[b]Department of Biomedical and Pharmaceutical Science, Graduate School, Kyung Hee University, Seoul 02447, Republic of Korea. E-mail: msohok@khu.ac.kr
[c]Department of Precision Medicine, Graduate School, Kyung Hee University, Seoul 02447, Republic of Korea. E-mail: jk.chembiologist@gmail.com
[d]Department of Anatomy and Neurobiology, College of Medicine, Kyung Hee University, Seoul 02447, Republic of Korea
[e]Medical Research Center for Bioreaction to Reactive Oxygen Species and Biomedical Science Institute, School of Medicine, Graduate School, Kyung Hee University, Seoul 02447, Republic of Korea
[f]Center for Converging Humanities, Kyung Hee University, Seoul 02447, Republic of Korea
[g]Department of Biomedical Science, Graduate School, Kyung Hee University, Seoul 02447, Republic of Korea

†Electronic supplementary information (ESI) available. See DOI: https://doi.org/10.1039/d4bm01368a

‡These authors contributed equally.

with oral administration and ultimately enhance patient compliance.[33,34] A few materials are currently used as transdermal delivery systems, such as microneedles, liposomes, and hydrogels, but distinct disadvantages are coined, such as causing skin tissue damage, low stability, low biocompatibility, and high production costs.[35–37]

Herein, we disclose a new transdermal delivery system for DNZ using a dimethylsiloxane-based polymeric material with high biocompatibility and stability that overcomes the drawbacks of traditional transdermal drug delivery materials, demonstrating its therapeutic applicability for suppressing AD symptoms in a mouse model *via* topical administration (Fig. 1). The polymer (TFA-siloxane polymer; T2 polymer) was prepared by the ring-opening polymerization of the monomer (TDOP; 2,2,5,5-tetramethyl-2,5-disila-1-oxacyclopentane) with trifluoroacetic acid (TFA), followed by the addition of ethanol (EtOH) to promote cross-linking reactions. DNZ was loaded into the T2 polymer by vortex mixing, and the resulting formulation (DNZ@T2) was then applied to the AD mouse model *via* topical administration. The DNZ@T2 formulation exhibited low cytotoxicity and non-significant *in vivo* toxicity. The results from the animal studies indicated improved spatial working memory and long-term memory formation compared to oral administration of DNZ, suggesting that this transdermal delivery strategy could offer an innovative approach to AD treatment. This research proposes a new direction in AD treatment and expands the medical applications of dimethylsiloxane-based polymers.

2. Materials and methods

2.1. Polymer preparation

The T2 polymer was synthesized *via* a ring-opening polymerization process using the TDOP monomer and trifluoroacetic acid (TFA). In a 25 mL round-bottom flask, 10 mL of TDOP (2,2,5,5-tetramethyl-2,5-disila-1-oxacyclopentane) and 1.5 mL of TFA were combined and stirred at 650 rpm for 48 h at 80 °C. The product was purified by washing with 10 mL of ethanol three times to eliminate any unreacted monomer and residual TDOP. The resulting polymer was then dried under vacuum for 24 h at 25 °C. ^{1}H NMR and ^{19}F NMR spectra were measured in $CDCl_3$ using a Bruker AVANCE III 500 MHz (USA) (Fig. S1 and S2†). [T2]: ^{1}H NMR (500 MHz, $CDCl_3$) δ 0.43, 0.41, 0.39, 0.07, 0.03; [TFA]: ^{1}H NMR (500 MHz, $CDCl_3$) δ 11.46, 0.40, 0.13, 0.09. [T2]: ^{19}F NMR (471 MHz, $CDCl_3$) δ −75.87, −75.96, −76.09; [TFA]: ^{19}F NMR (471 MHz, $CDCl_3$) δ −75.77, −75.82, −75.86.

2.2. Drug encapsulation efficiency of the T2 polymer

To determine the drug encapsulation efficacy of the T2 polymer, a stock solution (10 mg mL^{-1}, EtOH, 60 μL) of donepezil (DNZ) was added to the T2 polymer (200 μL). The final solution, containing both T2 polymer and DNZ, was mixed using a vortex mixer and subjected to vacuum for 2 h at 25 °C. After the incubation period, the resulting T2 polymer was washed three times with EtOH (1 mL), with vortexing, to remove any unloaded DNZ. The supernatants from each

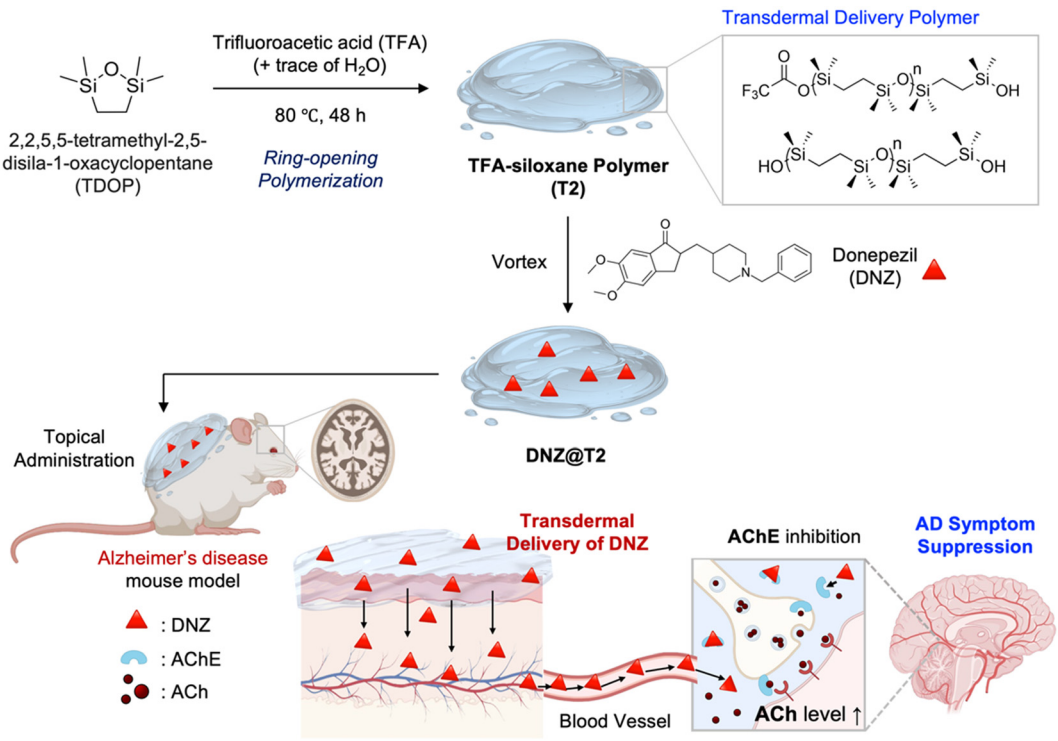

Fig. 1 Schematic illustration for the material preparation (T2, DNZ@T2) and the topical administration of DNZ@T2 to an Alzheimer's disease (AD) mouse model to confirm the transdermal delivery efficacy of donepezil.

washing step were collected for analysis. The encapsulation efficiency of DNZ was determined by measuring the absorption spectra of the supernatants using a spectrophotometer. The encapsulation efficiency was calculated using the equation (eqn (1)).

$$\text{Encapsulation efficiency}\,(\%) = [(\text{total drug} - \text{unloaded drug})/(\text{total drug})] \times 100 \quad (1)$$

2.3. Drug release test

The release profile of donepezil (DNZ) from the T2 polymer was analyzed using a spectrophotometer. DNZ-encapsulated T2 samples (DNZ@T2, 200 μL) were mixed with 1 mL of phosphate-buffered saline (PBS, pH 7.4) and incubated in a shaking incubator (200 rpm, 37 °C). At each time interval, supernatants were collected. The absorbance of DNZ in the supernatant was measured at 314 nm to determine the release profile.

2.4. Cell culture

b.End3 (mouse endothelial cell line) and HEK293 (human embryonic kidney cell line) cells were obtained from the Korean Cell Line Bank. Both cell lines were cultured in Dulbecco's modified Eagle's media (DMEM, Hyclone, USA), supplemented with 10% fetal bovine serum (FBS, Cat #SH30243.01, Hyclone, USA) and 1% penicillin–streptomycin (PS, Cat #15140122, Gibco, USA). All cell lines were maintained in a humidified atmosphere containing 5% CO_2 at 37 °C.

2.5. Cytotoxicity analysis

b.End3 and HEK293 cells were seeded in a 96-well cell culture plate (5×10^3 cells per mL, 100 μL per well) and incubated for 24 h at 37 °C. After incubation, the cells were treated with polymers (T2 or DNZ@T2) for 24 h. In the T2-treated group, cells were incubated with T2 polymer at final concentrations of 5%, 10%, and 20% (v/v) in the cell culture media. In the DNZ@T2-treated group, cells were treated with DNZ@T2 to achieve a final DNZ concentration of 100 μM, with the same T2 polymer concentrations of 5%, 10%, and 20% (v/v) in the culture media. Afterwards, the polymer was washed three times with DPBS, and cytotoxicity of the DNZ@T2 was evaluated using the Cell Counting Kit-8 (CCK-8) following the manufacturer's protocol.

2.6. Animals

Six-week-old male Balb/c nu/nu mice and Balb/c mice were obtained from DBL Co., Ltd (Incheon, Rep. of Korea). The mice were housed in groups of five per cage (27 × 22 × 14 cm) with free access to food and water in the animal room and were kept under a 12 h light/dark cycle (lights on from 07:30 to 19:30), with a constant temperature (23 ± 1 °C) and relative humidity (60 ± 10%). The mice were acclimated to the animal room for one week before the experiments. Animal treatment and maintenance were performed following the Animal Care and Use Guidelines of Kyung Hee University. All experimental protocols were approved by the Institutional Animal Care and Use Committee of Kyung Hee University (approval no.: KHSASP-22-024).

2.7. Skin penetration efficiency analysis

Balb/c nu/nu mice were randomly divided into four groups (n = 3 per group) as follows: (i) Oil Red O (OR)-treated group, (ii) OR-loaded T2 (OR@T2)-treated group, (iii) methylene blue (MB)-treated group, and (iv) MB-loaded T2 (MB@T2)-treated group. After the topical administration of each sample (100 μL, 24 h), the skin of each mouse was harvested and frozen using an optimal cutting temperature (OCT) compound to observe the cross-sectional views of the skin. Frozen skin samples were sectioned at 15 μm slices using a CM1510 cryostat microtome (Leica, Wetzlar, Germany) and placed on glass slides. The skin penetration efficiency was assessed using confocal laser scanning microscopy (CLSM, LSM-800, Carl Zeiss, Oberkochen, Germany). The confocal images of OR@T2 (red), MB@T2 (blue) were obtained under the excitation at 561 and 636 nm (laser power: 2.00 and 0.20%) with a detector (GaAsP, detector gain: 700 and 650 V; detection wavelength: 630–700 and 645–700 nm).

2.8. Hemolysis assay

Blood was collected from the hearts of the mice anaesthetized with isoflurane. Red blood cells (RBCs) were extracted from the blood by centrifugation at 4 °C (3000 rpm, 5 min) and washed twice with 1× PBS. [Positive control: 0.1% (working concentration) Triton X-100].[1] For the hemolysis assay, PBS (control), T2 (1 μM), or DNZ@T2 (1 μM) were mixed with 8% RBCs (in PBS) and incubated in a shaking incubator (200 rpm, 37 °C) for 1 h. After incubation, the mixture was centrifuged at 3000 rpm at 4 °C, and the supernatant was collected. Hemolysis was determined by measuring the absorbance of the supernatant at 450 nm.

2.9. *In vivo* toxicity analysis

Nine Balb/c mice were randomly divided into three groups as follows: (1) control group (non-treated group, n = 3), (2) T2 group (T2-treated group, n = 3), (3) DNZ@T2 group (DNZ@T2-treated, n = 3). Both T2 (50 μL) and DNZ@T2 (5 mg kg^{-1}, 50 μL) were administered transdermally to their respective groups for 7 days. On the 7th day, one hour after the final administration, blood was collected from all the mice, and they were then sacrificed. Organs, including the liver, kidney, spleen, thymus, and lymph nodes, were harvested for further analysis. Over the 7-day period, changes in body weight and food and water intake were recorded daily.

2.10. Behaviour tests for memory function assessment

To investigate the memory-improving effects of transdermally delivered DNZ, animal behavioral experiments were conducted using a scopolamine-induced memory impairment mouse model. DNZ was administered either orally (p.o.) or transdermally (t.d.) to the mice for 3 days, both before and during the behavioural testing. Scopolamine was injected intraperitone-

ally 30 min before each behavioural test to induce memory impairment. Details of the experimental setup are described in Fig. 5a. Learning and memory were evaluated using the Y-maze and the step-through passive avoidance test (PAT).[38] The Y-maze test was carried out in a three-arm horizontal maze. The number of arm entries and actual alternations (consecutive entries into all three arms) were recorded. The percentage of alternations was calculated using the following equation (eqn (2)):

$$\text{Alternation}\,(\%) = [(\text{number of alternations}) / (\text{total arm entries} - 2)] \times 100 \quad (2)$$

The PAT was conducted using a box divided into bright and dark compartments separated by a guillotine door. Each mouse was initially placed in the bright compartment. Upon opening the door, the mouse was allowed to enter the dark compartment. After the mouse fully entered the dark chamber, the guillotine door was closed, and a mild electrical foot shock (0.75 mA) was delivered for 3 s through the grid floor. 24 hours after the acquisition trial, the retention trial was conducted by placing the mouse back into the bright compartment. The time taken for the mouse to enter the dark chamber (latency) was recorded for a maximum of 300 s. Longer latency times indicated better memory retention.

2.11. Brain tissue collection and measurement of acetylcholine (ACh) levels

Mice were anesthetized, and their hippocampi were harvested through dissection 2 h after the dermal application of DNZ@T2 and 30 min after the scopolamine injection. The ACh levels in the hippocampal tissues were measured using assay kits (product no.: K615-100, BioVision, Milpitas, CA, USA) according to the manufacturer's protocol. The fluorescent intensity of the samples was measured using a FLUOstar Omega multimode microplate reader (BMG LABTECH, Ortenberg, Germany).

2.12. Statistical analysis

All statistical results were analyzed using Prism 8.0 software (GraphPad, La Jolla, California, USA).

3. Results and discussion

3.1. Materials characterization

The T2 polymer was synthesized *via* ring-opening polymerization of the TDOP monomer (10 mL) at 80 °C in the presence of TFA (1.5 mL) without a solvent. The resulting T2 polymer (200 μL) was mixed with a stock solution of DNZ (10 mg mL^{-1} in EtOH) (60 μL) using a vortex mixer and vacuumed for 2 h at 25 °C. After this period, the DNZ-loaded T2 polymer (named DNZ@T2) was washed three times with EtOH (1 mL) using vortexing to remove any unloaded DNZ. The loading efficiency of DNZ on the T2 polymer was determined through the standard curve of DNZ on EtOH (Fig. S3 and S4†). The results confirmed that approximately 80% of DNZ was loaded onto the T2 polymer. The DNZ@T2 was characterized using various analytical techniques (Fig. 2), including gel permeation chromatography (GPC), attenuated total reflectance Fourier Transform Infrared (ATR-FTIR) spectroscopy, thermos-gravimetric analysis (TGA), and viscosity measurements.

In the GPC analysis, the molecular weight of the T2 polymer was determined to be 17 675 g mol^{-1}, substantiating the formation of a high-molecular-weight polymer (Fig. 2a). In contrast, the monomeric state of TDOP exhibited a molecular weight of 186 g mol^{-1}, indicating that the T2 polymer comprises approximately 90 repeats of the dimethylsiloxane backbone. After confirming the high molecular weight of the T2 polymer, ATR-FTIR analysis was performed to verify the loading of DNZ into the T2 polymer. The ATR-FTIR analysis revealed the ν (C–H) peak of T2 polymer at 2800–3000 cm^{-1}, which was also observed in the DNZ@T2 formulation (Fig. 2b).[39] In addition, the ν (O–H) peak at 3558–3607 cm^{-1} and the ν (C═O) peak at 1681 cm^{-1} of DNZ were also present in the DNZ@T2 spectrum.[40,41] These results indicated that DNZ was successfully loaded into the T2 polymer, confirming the proper formation of DNZ@T2. Viscosity measurements of TDOP, T2 polymer, and DNZ@T2 indicated that both T2 and DNZ@T2 maintained consistent viscosity across a range of shear rates, while the monomer displayed shear-thinning behaviour (Fig. 2c). These results demonstrated that DNZ@T2 retained a similar viscosity after loading DNZ, proving its suitability for applications requiring consistent viscosity. These results were further supported by visual observation (Fig. 2d). As shown in the pictures when the vial was inverted, the contents did not easily spill due to their high viscosity, indicating that both T2 and DNZ@T2 exhibited similar viscosities. This behaviour differed from the viscosity of TDOP in its monomer form.

Next, TGA profiles were obtained for TDOP, T2 polymer, and DNZ@T2 under a nitrogen atmosphere (Fig. 2e). The TGA results demonstrated that the T2 polymer exhibited a greater weight loss than TDOP at higher temperatures, likely due to its more distinct polymer morphology. In addition, DNZ@T2 displayed a higher weight loss at around 400 °C compared to T2, indicating successful loading of DNZ. Lastly, the controlled release profile of DNZ from the T2 polymer was evaluated (Fig. 2f and S5†). DNZ@T2 (200 μL) was mixed with PBS (1 mL, pH 7.4) and incubated (200 rpm, 37 °C) to assess the release profile of DNZ. As a result, DNZ was released from the T2 polymer over approximately 22 days without burst release, representing that DNZ was stably loaded onto the T2 polymer. In addition, the high stability of DNZ@T2 in biological media was confirmed regarding the long-term hydrolysis of T2 polymer.

We compared the DNZ loading and releasing property of T2 polymer with hyaluronic acid (HA)-based hydrogel, a polymer among existing transdermal carriers used for various transdermal delivery, which is well utilized as a high molecular weight material similar to T2 polymer. As a result, the HA-based hydrogel showed high efficacy for DNZ loading, but it was

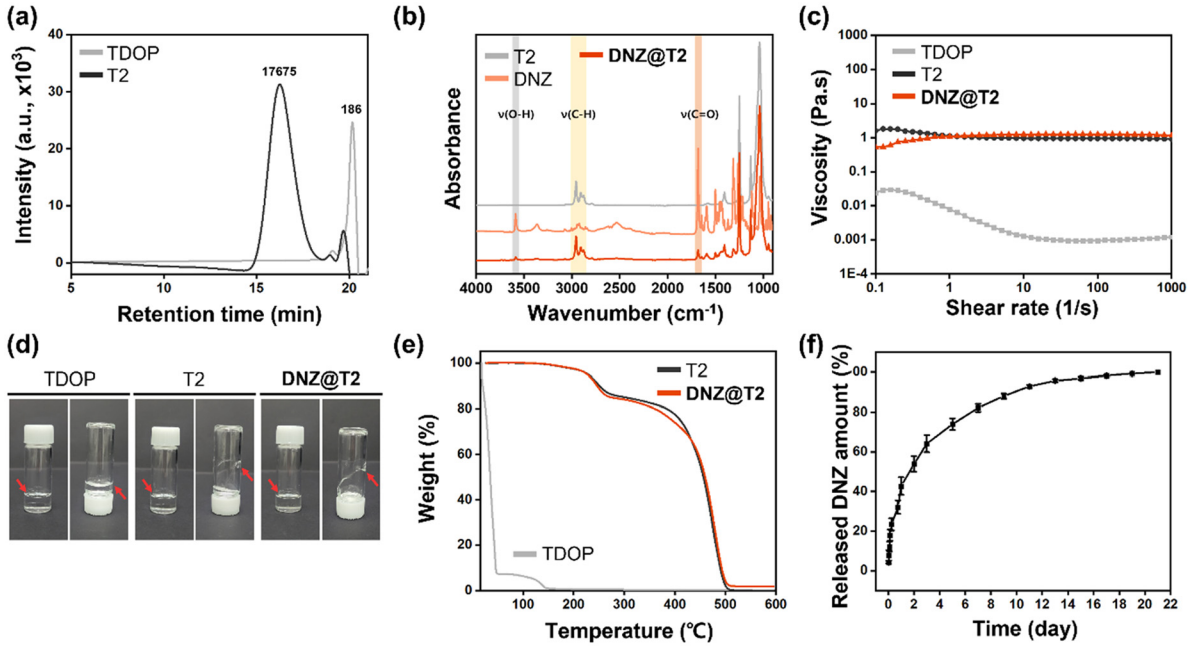

Fig. 2 (a) Gel-permeation chromatography (GPC) spectra of TDOP and T2 polymer. Unit: g mol^{-1}. (b) Attenuated total reflectance Fourier transform infrared (ATR-FTIR) spectra of T2 polymer, DNZ, and DNZ@T2. Symbols: ν = stretching. (c) Viscosity measurement as a function of shear rate for TDOP, T2 polymer, and DNZ@T2. The monomer exhibited shear-thinning behaviour, while both T2 polymer and DNZ@T2 maintained consistent viscosity. (d) Photographs of TDOP, T2 polymer, and DNZ@T2. Left: each series stood upright within the glass vial, right: each series stood inverted in the vial. The red arrow indicates the location of the polymer. (e) Thermogravimetric analysis (TGA) profiles of TDOP, T2 polymer, and DNZ@T2 under a nitrogen atmosphere. (f) Release profile of the DNZ from the DNZ@T2. The data are presented as means ± S.E.M. (n = 3).

immediately dissolved and released all the loaded DNZ when exposed to PBS due to its high hydrophilicity (Fig. S6†). In addition, DNZ-loaded HA(DNZ@HA) released DNZ immediately upon contact with the mouse skin, making it impossible to perform skin penetration analysis.

3.2. Skin permeability efficiency

Next, we conducted the skin permeability efficiency analysis of DNZ@T2. Complex mechanisms of the material's transdermal permeability property exist. In transdermal delivery, various factors could be considered, such as the balance between the hydrophilicity, hydrophobicity, and lipophilicity of the carrier, the molecular size above the appropriate level that prevents uptake into skin cells, and the morphological appearance of the substance.[42–44] The skin permeability properties of T2 polymer have been verified in these aspects in our previous paper.[45] In this study, we further verified the permeation effectiveness for DNZ transdermal delivery. To confirm the ability of DNZ@T2 to deliver DNZ into the bloodstream *via* the transdermal pathway, we loaded hydrophobic and hydrophilic fluorescent dyes (Oil Red O (OR) as the hydrophobic dye and methylene blue (MB) as the hydrophilic dye) into the T2 polymer to assess the transdermal delivery efficacy. Four sets were prepared for the treatment; (i) OR (20 mg in 100 μL EtOH), (ii) OR@T2 (20 mg in 100 μL T2 polymer), (iii) MB (20 mg in 100 μL EtOH), and (iv) MB@T2 (20 mg in 100 μL T2 polymer). Each formulation was applied to the back skin of mice. After 24 h, the mice were sacrificed, and the skin was cryo-sectioned. The skin penetration efficacy of the T2 polymer was evaluated using confocal laser scanning microscope (CLSM) imaging of the skin tissues. The results from the penetration efficacy experiment confirmed that the group treated with OR alone barely penetrated the skin. In contrast, OR@T2 demonstrated significantly greater penetration, visually confirming the enhanced delivery efficacy of the T2 polymer (Fig. 3a). This result was further supported by fluorescence intensity analysis (Fig. 3b). The group treated with OR@T2 exhibited higher overall fluorescence intensity compared to the group treated with OR alone, indicating that the substance effectively penetrated the epidermis and reached the hypodermis. This enhanced penetration was similarly observed for MB, where the T2 polymer facilitated improved transdermal delivery. Visual observations confirmed a marked increase in the skin penetration of MB facilitated by the T2 polymer (Fig. 3c). In addition, fluorescence intensity analysis demonstrated that MB gradually moved from the epidermis to the hypodermis, consistent with the results with the OR-treated group (Fig. 3d). These findings indicate that the T2 polymer exhibits high penetration efficacy for skin delivery with securing loaded drug, facilitating the transdermal movement of both hydrophilic or hydrophobic substances, enabling them to penetrate the hypodermal layer within approximately 24 h, which are representative advantages compared with known HA-based hydrogels.[46]

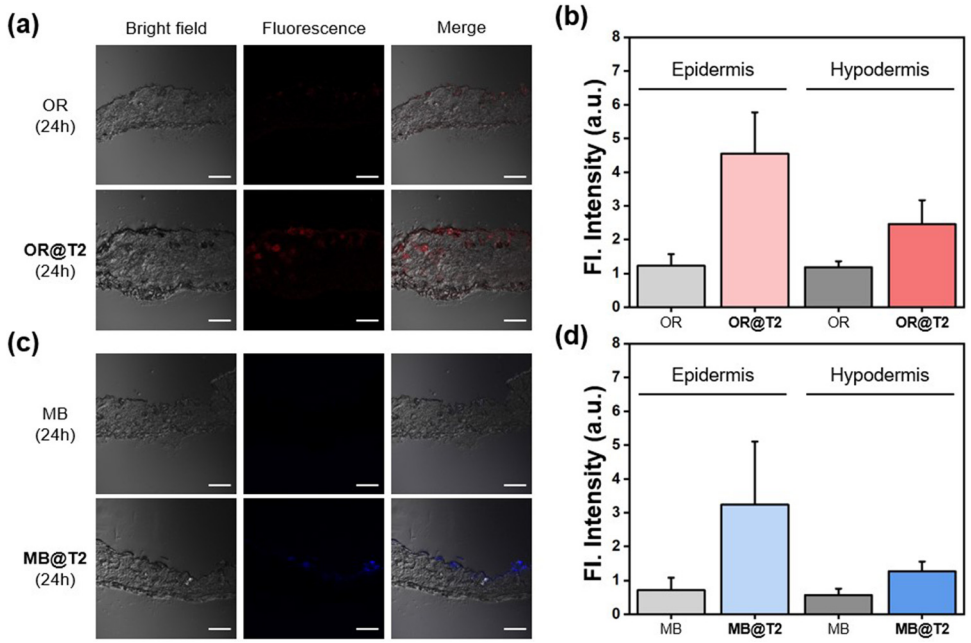

Fig. 3 (a and c) CLSM images of mouse back skin treated with OR/MB and OR@T2/MB@T2. Tissue samples collection time point after treatment: 24 h. The images display a bright field, fluorescence (red signal for OR and blue signal for MB), and merged images. Excitation and emission channel: OR (561 nm/630–700 nm), MB (636 nm/645–700 nm). Scale bar: 100 μm. (b and d) Quantification of fluorescence intensity in the epidermis and hypodermis layers of skin treated with OR/MB and OR@T2/MB@T2. Fluorescence intensity was analyzed using the Image-J program, and the values are presented as mean ± standard deviation.

3.3. *In vitro* and *in vivo* toxicity assessment

After establishing the enhanced skin permeability of the T2 polymer, we analyzed the toxicity of T2 and DNZ@T2 to confirm their safety for biomedical applications. The initial evaluation of toxicity was conducted on the b. End 3 cell line and HEK293 cell line, both of which are classified as normal cells (Fig. 4a and b). In this experiment, the treatment groups were divided into three categories: the T2 polymer (0.25, 0.5, 1 μM) treatment group, the DNZ@T2 (0.25, 0.5, 1 μM) treatment group, and the DNZ (100 μM) treatment group. The cell viability test results confirmed no significant differences compared to the control group across all treatment groups. Next, we confirmed the toxicity *in vivo* based on the results of the cytotoxicity analysis. We first performed hemolysis assays with the T2 polymer and DNZ@T2 at a concentration of 1 μM, a higher concentration that previously showed no toxicity at the cellular level (Fig. 4c). The hemolysis assay results indicated that hemolysis activity was significantly lower than that of the positive control group treated with Triton X-100, with no significant difference compared to the control group treated with PBS. Based on the results, the T2 polymer (1 μM) and DNZ@T2 (100 μM DNZ in 1 μM T2 polymer) were applied to the backs of balb/c nu/nu mice for 7 days to assess short-term toxicity. This was evaluated through observations of skin rash (Fig. S7†), body changes in weight (Fig. 4d), water and food intake change (Fig. 4e), and organ weight (Fig. 4f). The short-term toxicity results showed no gross changes in the skin of any mouse group, and there were no significant differences in body weight, water and food intake, and the weights of six organs (brain, heart, lung, liver, spleen, and kidney). The absence of weight changes in the liver, spleen, and kidneys, which are particularly sensitive to inflammatory changes, indicates that no inflammatory responses occurred. These short-term *in vivo* toxicity results demonstrated that both the T2 polymer and DNZ@T2 were sufficiently safe for application *in vivo*.

3.4. Therapeutic efficacy analysis

Based on the skin penetration efficacy and toxicity results of the T2 polymer, we evaluated the therapeutic efficacy of DNZ@T2 for the treatment of AD. To assess the effectiveness of DNZ through transdermal delivery, we established an AD mouse model by administering scopolamine based on the cholinergic hypothesis among various Alzheimer's hypotheses. To verify the therapeutic efficacy of DNZ@T2 using this cholinergic blockade AD mouse model, a series of animal behavioural experiments, including the Y-maze test, passive avoidance test (PAT), and acetylcholine level analysis, were conducted following the schedule in Fig. 5a. The concentration of DNZ was based on 5 mg kg^{-1}, which is the oral administration concentration of mice that safely induces memory improvement effects in AD research, and the low concentration of 1 mg kg^{-1} and the high concentration of 25 mg kg^{-1} were added to confirm the concentration-response results.[21,47] For the administration of DNZ@T2, the Balb/c mice were prepared by shaving the hair from their backs. The mice were then pre-

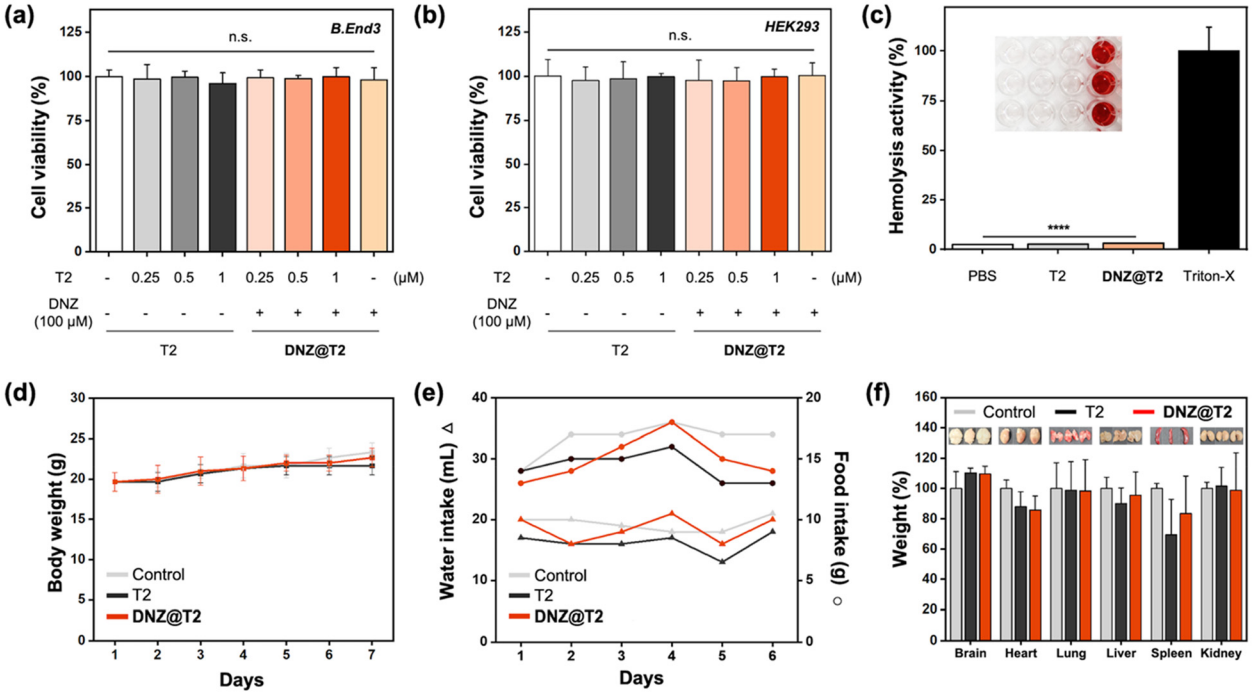

Fig. 4 (a and b) Cell viability assay results of b.End3 and HEK293 cells treated with different concentrations of T2 polymer and DNZ@T2. Data are presented as mean ± S.E.M. (n = 3). n.s.: non-significant difference. (c) Hemolysis activity assay results for PBS, T2 polymer, DNZ@T2, and Triton X-100 (positive control). The inset displays the visual results of the hemolysis test. Data are shown as means ± S.E.M. (n = 3). ****<0.001 compared to the Triton X-100 group. (d) Body weight measurements and (e) water/food intake over 7 days for the control (non-treated), T2 polymer, and DNZ@T2 groups. Mice were treated daily with 50 μL of samples (T2 polymer or DNZ@T2) applied to their backs and were monitored for 7 days. Data are presented as mean ± S.E.M. (n = 3). (f) Organ weight measurements for the brain, heart, lung, liver, spleen, and kidney, taken immediately after sacrifice on day 7 for the control (non-treated), T2 polymer, and DNZ@T2 groups. Data are presented as mean ± S.E.M. (n = 3).

treated with DNZ@T2 to visually observe the shedding of the substance over time. After administration, the mice were anaesthetized for 60 min to ensure complete penetration of the drug into the skin (Fig. 5b). To confirm the efficacy of transdermal delivery of DNZ *via* the T2 polymer for the treatment of AD, we designed two major sets; (i) comparing the therapeutic efficacy of oral administration *versus* transdermal delivery of DNZ without a transdermal carrier, (ii) assessing the efficacy of the T2 polymer as a transdermal delivery carrier for DNZ.

First, scopolamine and DNZ were administered orally and transdermally using the T2 polymer for 3 days to maximize the drug's half-life. Afterwards, the Y-maze test and PAT were performed to assess memory function. After the behavioural test, the mice were sacrificed and their hippocampi were harvested to analyze acetylcholine levels. The Y-maze experiment was conducted to check the working memory and short-term memory of the mice. The results indicated a trend toward memory improvement in both the DNZ-treated group (p.o.; per oral) and the DNZ@T2-treated group compared to the scopolamine-treated group (Fig. 5c). In particular, DNZ@T2 at a concentration of 25 mg kg^{-1} (DNZ) demonstrated a significant memory improvement compared to the scopolamine-treated group, similar to the effects observed with orally administered DNZ. On the other hand, the total arm entry results showed no significant difference among the groups, confirming that there was no tendency for hyperactivity related to the substance treatments (Fig. S8a†). This finding was also consistent with the PAT results, which assessed traumatic memory and long-term memory (Fig. 5d). Among them, both the DNZ-treated group (p.o.) and the DNZ@T2-treated group (at a concentration of 5 mg kg^{-1} of DNZ) exhibited significant memory improvement compared to the scopolamine-treated group. Additionally, there were no significant differences observed in the latency time on the acquisition day of the PAT experiment, further confirming that hyperactivity due to substance treatment did not occur (Fig. S8b†). The acetylcholine levels in the hippocampus of the mice, sacrificed after the PAT experiment, corroborated these behavioural results (Fig. 5e). Acetylcholine levels also exhibited similar improvements in the DNZ@T2 treatment group compared to the orally treated DNZ group, especially at a concentration of 5 mg kg^{-1} (DNZ), where a significant difference was confirmed against the group treated solely with scopolamine. These experimental results indicated that the transdermal delivery of DNZ *via* the T2 polymer had similar efficacy to the oral administration of DNZ, demonstrating that this method could have therapeutic potential in the treatment of AD. To further prove that the efficacy of this transdermal delivery system for treating AD was attributed to the T2 polymer, an additional experiment was conducted using DNZ

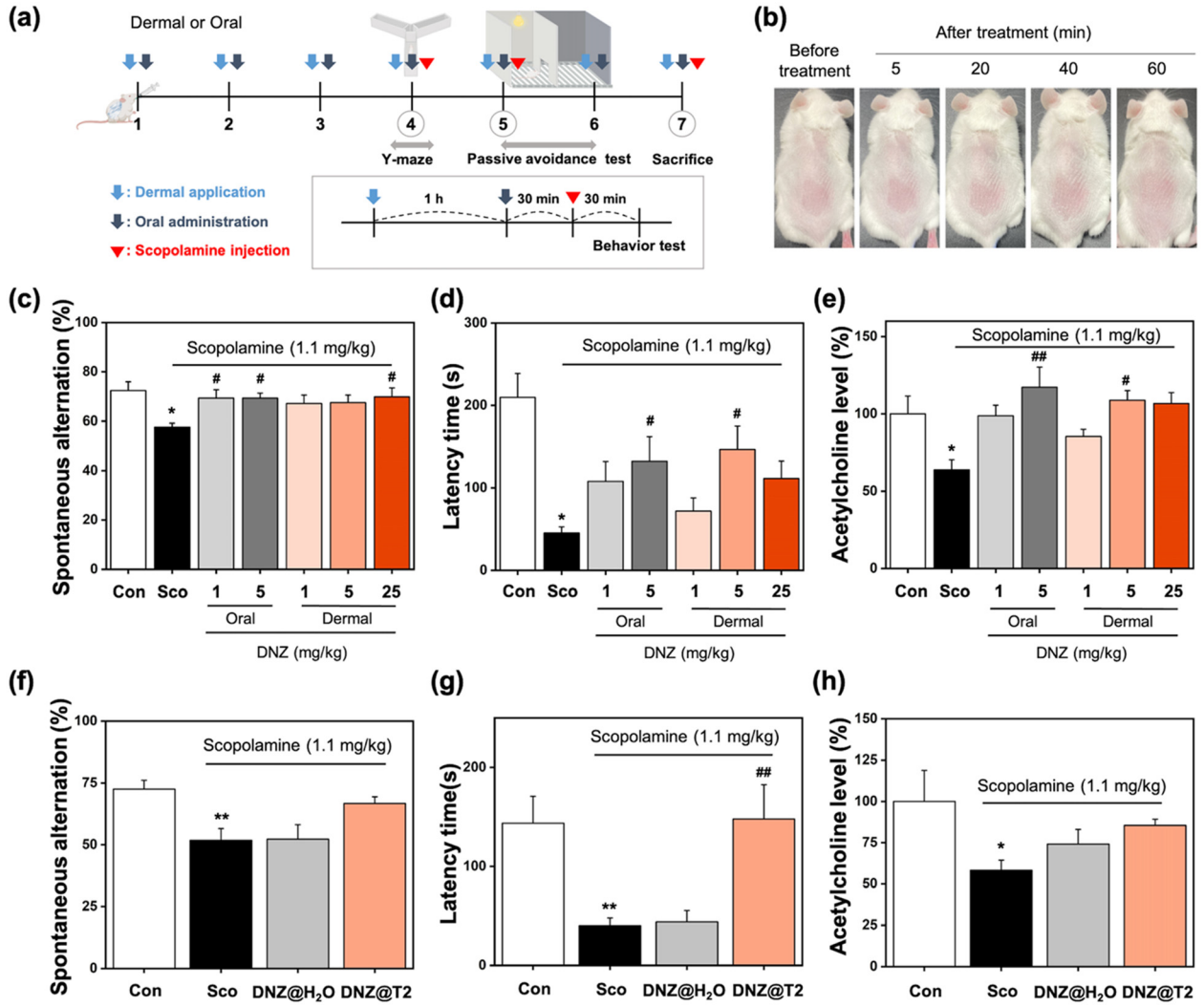

Fig. 5 (a) Experiment schedule for administration and behaviour testing. (b) Representative images after dermal application. The effect of DNZ@T2 on memory function was measured using the (c and f) Y-maze to measure spontaneous alternation (%), (d and g) passive avoidance test (PAT) to determine latency time (sec), and (e and h) acetylcholine levels (%) in the hippocampus. The data were analyzed using one-way ANOVA followed by Dunnett's multiple comparison test. #$p < 0.05$ and ##$p < 0.01$ *vs.* the normal group; *$p < 0.05$ and **$p < 0.01$ *vs.* the scopolamine-injected group.

dissolved in DI H_2O as a comparison group. In the Y-maze results, the DNZ@T2 group at a concentration of 5 mg kg^{-1} (DNZ) showed a tendency to improve memory compared to the scopolamine treatment group, while the treated with DNZ in DI H_2O did not exhibit any such tendency (Fig. 5f). The total arm entry results from the Y-maze test did not reveal any significant differences, confirming that there were no other effects from the substance treatments (Fig. S9a†). These differences in treatment efficacy were further supported by the results of the PAT (Fig. 5g). In the group treated with DNZ@T2, a significant increase in latency time was observed on the retention day compared to the scopolamine-treated group. However, no differences were observed in the group treated with DNZ dissolved in DI H_2O, reinforcing the therapeutic potential of DNZ@T2. In addition, the absence of variations in latency times on the acquisition day among all groups substantiates that the behavioural experimental results were attributed to the AD treatment efficacy of DNZ@T2 (Fig. S9b†). These behavioural outcomes were consistent with the acetylcholine levels in the hippocampus (Fig. 5h). Overall, the therapeutic efficacy results of transdermal delivery of DNZ@T2 in the scopolamine-induced AD mouse model demonstrate that DNZ@T2 can serve as a promising alternative administration method for AD. This approach yields similar efficacy to oral administration of DNZ, potentially enhancing patient adherence and overall treatment success.

4. Conclusions

In this study, we aimed to develop a novel therapeutic formulation of DNZ for transdermal administration to achieve

enhanced treatment convenience for AD patients. We disclosed a DNZ-loaded T2 polymer system (named DNZ@T2), which demonstrated promising properties for transdermal drug delivery based on its high biocompatibility. Our findings confirmed that DNZ@T2 can deliver various substances transdermally with higher efficiency. In AD mouse model studies, DNZ@T2 exhibited superior therapeutic efficacy compared to oral DNZ administration, improving memory function and increasing acetylcholine levels in the hippocampus in a scopolamine-induced cholinergic blockade AD mouse model. The memory-enhancing effects of DNZ@T2 were comparable to those observed with oral DNZ, proving the efficacy of this delivery method. Furthermore, the T2 polymer demonstrated its ability to serve as an effective vehicle for the delivery of DNZ, highlighting its potential in the treatment of AD. Through transdermal drug delivery utilizing T2 polymer, DNZ can effectively overcome side effects such as noncompliance and drug intake refusal in AD patients. In addition, considering the current drug properties as polymer, it can be developed in various forms such as patches or ointments for AD patients, and through this, it can help improve memory through transdermal delivery (Fig. S10†). We are confident that our newly developed DNZ@T2 will offer greater convenience and therapeutic efficacy in the management of AD, addressing the challenges associated with conventional oral treatments.

Ethical statement

Animal treatment and maintenance were performed following the Animal Care and Use Guidelines of Kyung Hee University. All experimental protocols were approved by the Institutional Animal Care and Use Committee of Kyung Hee University (approval no.: KHSASP-22-024).

Author contributions

Jihyun Lee: Methodology, investigation, visualization, writing – original draft, writing – review & editing. In Gyoung Ju: Methodology, investigation, visualization. Yeon-Jin Lim: Investigation. Jin Hee Kim: Investigation. Seungmin Lee: Investigation. Yujin Choi: Investigation. Myung Sook Oh: Supervision. Jaehoon Kim: Conceptualization, methodology, supervision, writing – original draft, writing – review & editing. Dokyoung Kim: Conceptualization, funding acquisition, project administration, supervision, writing – review & editing.

Data availability

The authors confirm that the data supporting the findings of this study are available within the article and its ESI.† The data that support the findings of this study are available from the corresponding author, [D. Kim], upon reasonable request.

Conflicts of interest

The authors declare the following competing financial interest (s): the authors are listed as inventors on a pending patent application related to the technology described in this work.

Acknowledgements

This work was supported by grants from the National Research Foundation (NRF) of Korea (2022-R1F1A1069954). This research was also supported by the Core Research Institute (CRI) Program, the Basic Science Research Program through the NRF of Korea, the Ministry of Education (2018-R1A6A1A03025124), and the Bio & Medical Technology Development Program of the NRF of Korea (MSIT) (RS-2024-00439078). We acknowledge a grant of the Korea Health Technology R&D Project through the Korea Health Industry Development Institute (KHIDI), funded by the Ministry of Health & Welfare, Republic of Korea (HI23C1263). We are grateful for the advice and financial support from our collaborators, Mr Jinwoo Ahn and Mr Jucheol Lee (Dasan Pharmaceutical Co., Ltd, Rep. of Korea).

References

1 J. Kim, H. Um, N. H. Kim and D. Kim, *Bioact. Mater.*, 2023, **24**, 497–506.
2 P. Scheltens, B. De Strooper, M. Kivipelto, H. Holstege, G. Chételat, C. E. Teunissen, J. Cummings and W. M. van der Flier, *Lancet*, 2021, **397**, 1577–1590.
3 P. Scheltens, K. Blennow, M. M. Breteler, B. De Strooper, G. B. Frisoni, S. Salloway and W. M. Van der Flier, *Lancet*, 2016, **388**, 505–517.
4 J. Kim and D. Kim, *Bull. Korean Chem. Soc.*, 2022, **43**, 78–82.
5 X.-Y. Liu, L.-P. Yang and L. Zhao, *World J. Stem Cells*, 2020, **12**, 787.
6 C. Arber, C. Lovejoy and S. Wray, *Alzheimers Res. Ther.*, 2017, **9**, 1–17.
7 A.-M. Tolppanen, H. Taipale, M. Koponen, P. Lavikainen, A. Tanskanen, J. Tiihonen and S. Hartikainen, *BMJ Open*, 2016, **6**, e012100.
8 E. S. Oh, P. B. Rosenberg, G. B. Rattinger, E. A. Stuart, C. G. Lyketsos and J. M. S. Leoutsakos, *J. Am. Geriatr. Soc.*, 2021, **69**, 955–963.
9 P. Nilsson, N. Iwata, S. I. Muramatsu, L. O. Tjernberg, B. Winblad and T. C. Saido, *J. Cell. Mol. Med.*, 2010, **14**, 741–757.
10 B. Combs, A. Kneynsberg and N. M. Kanaan, *Gene Therapy for Neurological Disorders: Methods and Protocols*, 2016, pp. 339–366.
11 M. A. Parra, S. Abrahams, K. Fabi, R. Logie, S. Luzzi and S. D. Sala, *Brain*, 2009, **132**, 1057–1066.
12 M. A. Parra, S. Abrahams, R. H. Logie, L. G. Méndez, F. Lopera and S. Della Sala, *Brain*, 2010, **133**, 2702–2713.

13 J. L. Muir, *Pharmacol., Biochem. Behav.*, 1997, **56**, 687–696.
14 S. Lombardo and U. Maskos, *Neuropharmacology*, 2015, **96**, 255–262.
15 H. R. Parri, C. M. Hernandez and K. T. Dineley, *Biochem. Pharmacol.*, 2011, **82**, 931–942.
16 E. Giacobini, *Neurochem. Res.*, 2003, **28**, 515–522.
17 G. Marucci, M. Buccioni, D. Dal Ben, C. Lambertucci, R. Volpini and F. Amenta, *Neuropharmacology*, 2021, **190**, 108352.
18 R. M. Lane, M. Kivipelto and N. H. Greig, *Clin. Neuropharmacol.*, 2004, **27**, 141–149.
19 H. Sugimoto, Y. Yamanish, Y. Iimura and Y. Kawakami, *Curr. Med. Chem.*, 2000, **7**, 303–339.
20 D. Galimberti and E. Scarpini, *Expert Opin. Invest. Drugs*, 2016, **25**, 1181–1187.
21 J. Kim, Y. H. Seo, J. Kim, N. Goo, Y. Jeong, H. J. Bae, S. Y. Jung, J. Lee and J. H. Ryu, *J. Ethnopharmacol.*, 2020, **259**, 112843.
22 N. Tsuno, *Expert Rev. Neurother.*, 2009, **9**, 591–598.
23 R. Howard, R. McShane, J. Lindesay, C. Ritchie, A. Baldwin, R. Barber, A. Burns, T. Dening, D. Findlay and C. Holmes, *N. Engl. J. Med.*, 2012, **366**, 893–903.
24 Z. Q. Zhao, B. Z. Chen, X. P. Zhang, H. Zheng and X. D. Guo, *Mol. Pharmaceutics*, 2021, **18**, 2482–2494.
25 A. Calhoun, C. King, R. Khoury and G. T. Grossberg, *Expert Opin. Pharmacother.*, 2018, **19**, 1711–1717.
26 R. H. Affoo, N. Foley, J. Rosenbek, J. Kevin Shoemaker and R. E. Martin, *J. Am. Geriatr. Soc.*, 2013, **61**, 2203–2213.
27 N. Bassil and G. T. Grossberg, *CNS Drugs*, 2009, **23**, 293–307.
28 M.-C. Kearney, E. Caffarel-Salvador, S. J. Fallows, H. O. McCarthy and R. F. Donnelly, *Eur. J. Pharm. Biopharm.*, 2016, **103**, 43–50.
29 I. Mendes, A. Ruela, F. Carvalho, J. Freitas, R. Bonfilio and G. Pereira, *Colloids Surf., B*, 2019, **177**, 274–281.
30 W. Y. Jeong, M. Kwon, H. E. Choi and K. S. Kim, *Biomater. Res.*, 2021, **25**, 24.
31 S. Ruan, Y. Zhang and N. Feng, *Biomater. Sci.*, 2021, **9**, 8065–8089.
32 H. Labie and M. Blanzat, *Biomater. Sci.*, 2023, **11**, 4073–4093.
33 D. Woitalla, J. Kassubek, L. Timmermann, T. Lauterbach, R. Berkels, F. Grieger and T. Mueller, *Parkinsonism Relat. Disord.*, 2015, **21**, 199–204.
34 T. Tanner and R. Marks, *Sking Res. Technol.*, 2008, **14**, 249–260.
35 C. Wu, Q. Yu, C. Huang, F. Li, L. Zhang and D. Zhu, *Acta Pharm. Sin. B*, 2024, DOI: **10.1016/j.apsb.2024.08.013**.
36 M. S. Kapoor, A. D'Souza, N. Aibani, S. S. Nair, P. Sandbhor, D. Kumari and R. Banerjee, *Sci. Rep.*, 2018, **8**, 16122.
37 H. Lu, W. Shi, F. Zhao, W. Zhang, P. Zhang, C. Zhao and G. Yu, *Adv. Funct. Mater.*, 2021, **31**, 2101036.
38 H. J. Bae, J. Kim, S. J. Jeon, J. Kim, N. Goo, Y. Jeong, K. Cho, M. Cai, S. Y. Jung and K. J. Kwon, *J. Ethnopharmacol.*, 2020, **258**, 112923.
39 B. Ramaganthan, M. Gopiraman, L. O. Olasunkanmi, M. M. Kabanda, S. Yesudass, I. Bahadur, A. S. Adekunle, I. B. Obot and E. E. Ebenso, *RSC Adv.*, 2015, **5**, 76675–76688.
40 D. Wang, K. Gulyuz, C. N. Stedwell and N. C. Polfer, *J. Am. Soc. Mass Spectrom.*, 2011, **22**, 1197–1203.
41 A. Gencturk and A. S. Sarac, *Int. J. Electrochem. Sci.*, 2016, **11**, 111–125.
42 C. Richard, S. Cassel and M. Blanzat, *RSC Adv.*, 2021, **11**, 442–451.
43 S.-Y. Chen, X.-X. Xu, X. Li, N.-B. Yi, S.-Z. Li, X.-C. Xiang, D.-B. Cheng and T. Sun, *Biomater. Sci.*, 2022, **10**, 6642–6655.
44 Q. Tian, P. Quan, L. Fang, H. Xu and C. Liu, *Int. J. Pharm.*, 2021, **608**, 121082.
45 R. H. Kang, N. H. Kim and D. Kim, *Chem. Eng. J.*, 2022, **440**, 135989.
46 H.-Y. Lee, C.-H. Hwang, H.-E. Kim and S.-H. Jeong, *Carbohydr. Polym.*, 2018, **186**, 290–298.
47 J. Kim, J. Kim, Z. Huang, N. Goo, H. J. Bae, Y. Jeong, H. J. Park, M. Cai, K. Cho and S. Y. Jung, *Biomol. Ther.*, 2019, **27**, 327.

